J. Phys. B: At. Mol. Opt. Phys. **32** (1999) 1739–1754. Printed in the UK PII: S0953-4075(99)00174-1

Theoretical study of electron-impact excitation of H(1s) into the $n \leqslant 4$ states using a two-dimensional R-matrix propagator

K M Dunseath, M Terao-Dunseath, M Le Dourneuf and J-M Launay

Laboratoire PALMS (UMR 6627 du CNRS–Université de Rennes 1), Campus de Beaulieu, Université de Rennes I, 35042 Rennes Cedex, France

Received 16 December 1998, in final form 25 January 1999

Abstract. Electron-impact excitation of the ground state of hydrogen into the $n \leqslant 4$ states is studied by propagating the R-matrix in the two radial dimensions. Integral cross sections and resonance parameters are presented for collision energies from 0.75 Ryd (the $n = 2$ threshold) up to 0.96 Ryd (the $n = 5$ threshold). Below the $n = 3$ threshold, there is very good agreement with results from other methods and with experimental data. Between the $n = 3$ and $n = 4$ thresholds, integral cross sections are in better agreement with those of a coupled pseudostate method than with those of the J-matrix method, while resonance parameters are in good agreement with those of a 15-state R-matrix calculation.

1. Introduction

In a previous paper (Dunseath *et al* 1996, to be referred to as I), we developed a method of solving the two-electron Schrödinger equation by propagating the inverse of the logarithmic derivative matrix or R-matrix in two dimensions. The main feature of this method is the subdivision of the two-electron configuration space into a number of elementary domains, in each of which the wavefunction for the collision system is expanded in a local basis. This piecewise representation of the exact wavefunction allows an accurate treatment of an extended region of configuration space. This is particularly important for the study of processes involving diffuse states, such as the excitation of low-lying states into Rydberg states. The method is able to incorporate a large set of target states and pseudostates representing highly excited levels and the continuum of the target. These play an important role even at low energies by influencing the distribution of flux amongst the elastic and inelastic channels (see for example Callaway 1982, Fon *et al* 1994, Konovalov and McCarthy 1994, Odgers *et al* 1995, Bray *et al* 1996, Dunseath *et al* 1997).

In I, we applied the two-dimensional (2D) R-matrix propagator to the study of electron–hydrogen scattering, calculating phase shifts, resonance parameters and cross sections for collision energies up to the $n = 3$ threshold. We established the stability, efficiency and accuracy of the method by comparing with the results of other accurate calculations such as those using the finite-difference propagation (Wang and Callaway 1994), the finite-element (Shertzer and Botero 1994), convergent close-coupling (Bray and Stelbovics 1992) and intermediate-energy R-matrix (Scholz *et al* 1988) methods. We also reported some preliminary results for $^1S^e$ scattering up to the $n = 5$ threshold. The purpose of this paper is to present the results of a full calculation for this energy range. The effect of including highly excited states and the continuum of the target are even more important at these higher energies.

0953-4075/99/071739+16$19.50

Cross sections for excitation into states with $n \geqslant 3$ are needed in a number of areas. In astrophysics for example, accurate data are required in order to understand polarization in Hα spectral lines observed in solar flares (Aboudarham *et al* 1992). These cross sections are difficult to measure and to the best of our knowledge, no experiments have been performed for excitation into the $n \geqslant 3$ target states in this energy range. On the other hand, there are few theoretical data, due to the necessity of using very large bases in order to represent accurately the scattering wavefunction over a large region of the configuration space. It is precisely for this type of problem that the 2D R-matrix propagator is best suited.

The outline of this paper is as follows. In section 2 we summarize the method of propagating the R-matrix in two dimensions. We then present our results for integral cross sections and resonance parameters, considering separately the energy ranges between two thresholds. Between the $n = 2$ and $n = 3$ thresholds we make a detailed comparison with the results of other accurate calculations and with experimental data. There are not many other theoretical studies above the $n = 3$ threshold, which limits comparison.

We use atomic units except where otherwise stated.

2. R-matrix propagation in two dimensions

The 2D R-matrix propagation method is described in detail in I. We give only a brief outline here. The key idea is to solve the two-electron Schrödinger equation by partitioning the range of the radial coordinates r_1, r_2 of both electrons into a number of sectors. In a sector $s = [a_{s-1}, a_s]$, we define a set of orbitals $u^{(s)}_{n\ell}(r)$ with angular momentum ℓ as solutions of the eigenvalue problem

$$\left(-\frac{1}{2}\left[\frac{\mathrm{d}^2}{\mathrm{d}r^2} + \delta(r - a_{s-1})\frac{\mathrm{d}}{\mathrm{d}r} - \delta(r - a_s)\frac{\mathrm{d}}{\mathrm{d}r}\right] - \frac{Z}{r} + \frac{\ell(\ell+1)}{2r^2} - \epsilon_{n\ell}\right) u^{(s)}_{n\ell}(r) = 0. \tag{1}$$

We expand $u^{(s)}_{n\ell}(r)$ in a basis of N_P Legendre polynomials $P_n(x)$, with $x = (2r - a_s - a_{s-1})/(a_s - a_{s-1})$. In the first sector ($s = 1$), which contains the origin ($a_0 = 0$), we use the non-orthogonal basis $r\,P_n(x)$ where the factor r ensures that the eigenfunctions are regular at the origin.

The partitioning of the radial coordinates defines a decomposition of the two-electron configuration space into a number of elementary domains (see figure 1). For given total orbital momentum L, spin S and parity π, a discrete R-matrix basis is obtained in each domain (s, s') by solving the eigenvalue problem

$$(H + L_{\mathrm{B}}^{(s,s')} - E_k^{(s,s')})\Psi_k^{(s,s')} = 0, \tag{2}$$

with

$$H = -\frac{1}{2}\frac{\mathrm{d}^2}{\mathrm{d}r_1^2} - \frac{1}{2}\frac{\mathrm{d}^2}{\mathrm{d}r_2^2} - \frac{Z}{r_1} - \frac{Z}{r_2} + \frac{\ell_1(\ell_1+1)}{2r_1^2} + \frac{\ell_2(\ell_2+1)}{2r_2^2} + \frac{1}{r_{12}}. \tag{3}$$

Hermiticity in the current domain is ensured by inclusion of the Bloch operator

$$L_{\mathrm{B}}^{(s,s')} = \frac{1}{2}[\delta(r_1 - a_s) - \delta(r_1 - a_{s-1})]\frac{\mathrm{d}}{\mathrm{d}r_1} + \frac{1}{2}[\delta(r_2 - a_{s'}) - \delta(r_2 - a_{s'-1})]\frac{\mathrm{d}}{\mathrm{d}r_2}. \tag{4}$$

In a diagonal domain the eigenfunctions $\Psi_k^{(s,s)}$ are expanded for each spin as

$$\Psi_k^{(s,s)} = \sum_{\substack{n_1\ell_1 \\ n_2\ell_2}} \alpha_{n_1\ell_1 n_2\ell_2 k}\mathcal{A}u^{(s)}_{n_1\ell_1}(r_1)u^{(s)}_{n_2\ell_2}(r_2)\mathcal{Y}^{LM_L}_{\ell_1\ell_2}(\Omega_1, \Omega_2), \tag{5}$$

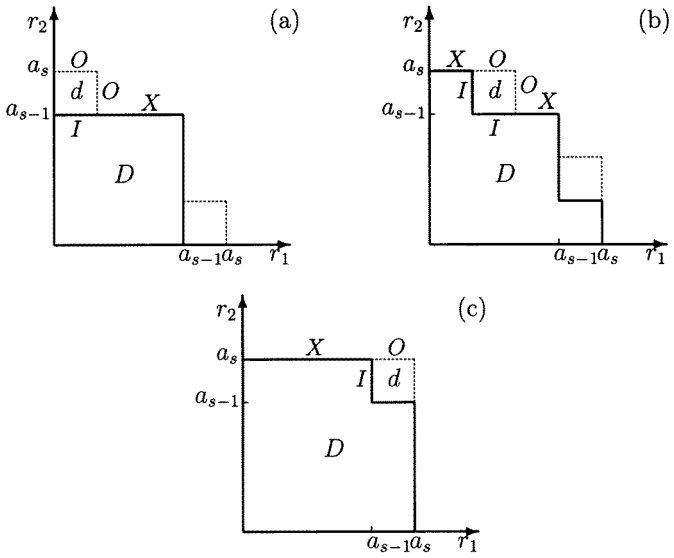

Figure 1. Subdivision of the 2D configuration space into elementary domains and the labelling scheme for each side of a typical domain. In (*a*) the domain d is being added to the domain D, boundary $X + I$, to give a domain D', boundary $X + O$. By symmetry, we need only consider half of the (r_1, r_2) plane; we choose to work in the upper half. The input border I consists of only one side as the R-matrix is zero when $r_1 = 0$. In (*b*) the domain d does not lie on an edge or on the diagonal; in this case both the input and output borders I and O consist of two sides. In (*c*) the domain d lies on the diagonal; by symmetry we need only consider one side of the input and output borders, provided that we multiply the elements of the corresponding R-matrix by two.

where $\mathcal{A}$ is the (anti)symmetrization operator and

$$\mathcal{Y}^{LM_L}_{\ell_1\ell_2}(\Omega_1, \Omega_2) = \sum_{m_1 m_2} (\ell_1 m_1 \ell_2 m_2 | L M_L) Y_{\ell_1 m_1}(\Omega_1) Y_{\ell_2 m_2}(\Omega_2),$$

where $(\ell_1 m_1 \ell_2 m_2 | L M_L)$ are Clebsch–Gordan coefficients and $Y_{\ell m}(\Omega)$ are spherical harmonics. In off-diagonal domains, where the two coordinates r_1 and r_2 span different subspaces, there is no exchange contribution to the matrix elements. The eigenvalue problem is therefore independent of the total spin S, and is solved once using the unsymmetrized expansion

$$\Psi^{(s,s')}_k = \sum_{\substack{n_1\ell_1 \\ n_2\ell_2}} \alpha_{n_1\ell_1 n_2\ell_2 k} u^{(s)}_{n_1\ell_1}(r_1) u^{(s')}_{n_2\ell_2}(r_2) \mathcal{Y}^{LM_L}_{\ell_1\ell_2}(\Omega_1, \Omega_2). \tag{6}$$

In expansions (5) and (6), the two-electron basis is built from the first N_O solutions of (1) for each orbital momentum. The remaining $N_P - N_O$ orbitals are included in the Buttle correction which accounts approximately for the terms omitted in the two-electron basis (see I). The coefficients in these expansions are determined by diagonalizing the two-electron Hamiltonian (3) in the elementary domain. Elementary R-matrices relating the radial functions to their derivatives on the surface of the domain can then be constructed.

Given the R-matrix $\boldsymbol{R}^D$ on the boundary $X + I$ of a domain D (see figure 1), the R-matrix $\boldsymbol{R}^{D'}$ on the boundary $X + O$ of a domain $D' = D + d$ may be obtained using the propagation

relations

$$\begin{aligned}
\boldsymbol{R}^{D'}_{OO} &= \boldsymbol{r}_{OO} - \boldsymbol{r}_{OI}(\boldsymbol{r}_{II} + \boldsymbol{R}^{D}_{II})^{-1}\boldsymbol{r}_{IO} \\
\boldsymbol{R}^{D'}_{OX} &= \boldsymbol{r}_{OI}(\boldsymbol{r}_{II} + \boldsymbol{R}^{D}_{II})^{-1}\boldsymbol{R}^{D}_{IX} \\
\boldsymbol{R}^{D'}_{XO} &= \boldsymbol{R}^{D}_{XI}(\boldsymbol{r}_{II} + \boldsymbol{R}^{D}_{II})^{-1}\boldsymbol{r}_{IO} \\
\boldsymbol{R}^{D'}_{XX} &= \boldsymbol{R}^{D}_{XX} - \boldsymbol{R}^{D}_{XI}(\boldsymbol{r}_{II} + \boldsymbol{R}^{D}_{II})^{-1}\boldsymbol{R}^{D}_{IX},
\end{aligned} \tag{7}$$

where $\boldsymbol{r}$ is the R-matrix evaluated on the four sides of the domain d.

The 2D R-matrix is propagated out to the boundary of a global square domain D_{out} defined by $r_1, r_2 \leqslant r_{\text{out}}$, where the exchange between the two electrons becomes negligible for the process of interest. We then define a set of target box states by diagonalizing the one-electron Hamiltonian (1) in the global sector $[0, r_{\text{out}}]$ using a basis of Legendre polynomials multiplied by r. The size of this basis depends on r_{out}. This procedure yields a discrete set of functions of which the lowest correspond very precisely to the first hydrogenic bound states, while the others are pseudostates representing highly excited states and the continuum. The channels involving pseudostates are asymptotically closed in the energy range considered here. They can, however, interact strongly with the open channels through short-range couplings, greatly influencing the final distribution of flux as can be seen when comparing calculations with and without pseudostates (see below).

Beyond r_{out} the scattering problem is solved within the close-coupling formalism (see, for example, Burke and Noble 1995). At the boundary r_{out}, the R-matrix $\mathcal{R}$ in the close-coupling basis is obtained from the R-matrix $\boldsymbol{R}$ in the 2D propagation basis by projecting the orbitals $u^{(s)}_{n\ell}(r)$ in each sector onto the target box states. The number of target box states retained in the close-coupling expansion depends on the collision energy. We have found that it is sufficient to retain those whose energies are up to 1.5 times the collision energy. The matrix $\mathcal{R}$ is then propagated in one dimension using a method developed by Light and Walker (1976), out to a distance r_{asy} where it is matched to a set of independent asymptotic solutions propagated inwards by an analytic expansion method (Gailitis 1976). This provides the K-matrix from which all quantities of interest can be obtained.

The division of configuration space into sub-regions in each of which the exact wavefunction for the system is approximated by a local set of functions (usually polynomials) is at the heart of finite-element methods (FEM). Shertzer and Botero (1994) have applied this approach to electron–hydrogen scattering. There are, however, some important differences between the 2D R-matrix propagator and the FEM. In the latter, the radial functions and their derivatives are propagated for each collision energy by imposing continuity across the element boundaries. The current method has the advantage that the computationally expensive operation of diagonalizing the Hamiltonians in each domain is independent of the collision energy. Furthermore, these diagonalizations can be performed in parallel over the domains. Finally, the propagation involves only one matrix inversion and several matrix multiplications which can be performed very efficiently.

3. Results and discussion

In order to calculate cross sections for excitation into states with principal quantum number $n \leqslant 4$ up to the $n = 5$ threshold, it is necessary to consider a region of the two-electron configuration space enveloping the $n = 5$ states. We actually extended this region out to 100 a_0. The radial coordinate of each electron is divided into 10 sectors of 10 a_0, with a basis of 40 Legendre polynomials per angular momentum used to define a set of orbitals, of which the lowest 15 are used in the two-electron basis. For each angular momentum, 80 basis functions are used to diagonalize the one-electron Hamiltonian (1) in the global sector $[0, 100\ a_0]$. A

total of 90 box states (20 s, 19 p, 18 d, 17 f, 16 g) are retained in the close-coupling expansion, more than enough to ensure convergence. Of these, 35 states have negative energies and the lowest 15 correspond precisely to the $n \leqslant 5$ states of hydrogen. No pseudo-resonances occur at the collision energies considered in this paper. Partial waves up to $L = 8$ are included, ensuring that the excitation cross sections are converged.

3.1. Between the $n = 2$ and $n = 3$ thresholds

There exists a large number of calculations of integral cross sections for the 1s–1s, 1s–2s and 1s–2p transitions at energies between the $n = 2$ and $n = 3$ thresholds. Callaway (1982) performed an 18-state variational close-coupling calculation using pseudostates (which we denote by CPS) whose results are in excellent agreement with the experimental values of Williams (1988). These have since become a benchmark against which new results are often compared. Of these, we may cite calculations using the J-matrix (Konovalov and McCarthy 1994), intermediate energy R-matrix (IERM, Odgers *et al* 1995, 1996), R-matrix with pseudostates (RMPS, Bartschat *et al* 1996) and convergent close-coupling (CCC, Bray *et al* 1996) methods. These have in common the introduction of a large number of pseudostates representing highly excited states and the continuum of the target. In contrast, a 15-state R-matrix calculation (Aggarwal *et al* 1991) which includes all the physical $n \leqslant 5$ states but no pseudostates yields elastic cross sections 6–7% lower than those of the CPS calculation while the excitation cross sections are of the order of 10% higher.

We present in figure 2 the results of a calculation using the 2D R-matrix propagator for excitation into the $n = 2$ states. There is excellent agreement with the experimental values

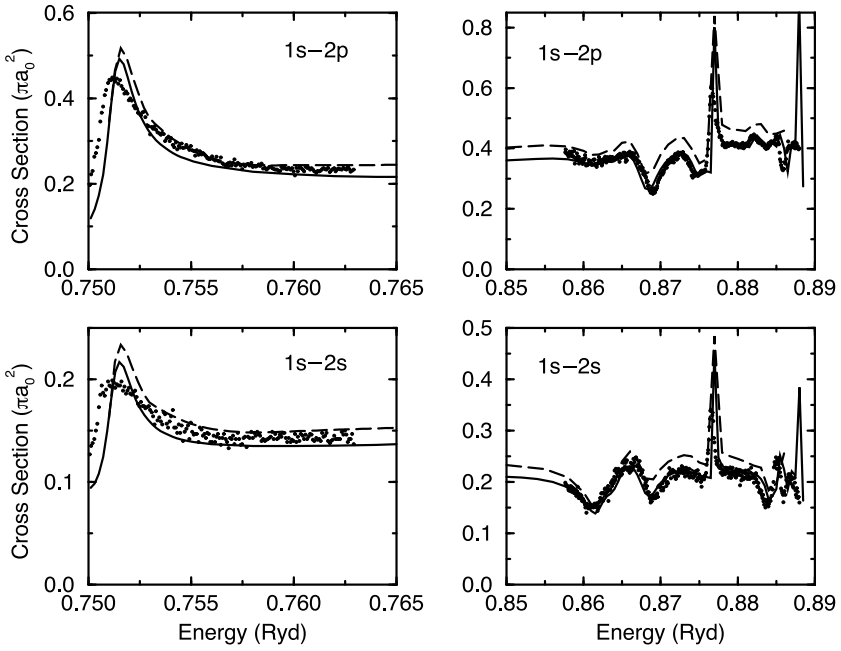

Figure 2. Integral cross sections for excitation of the ground state into the $n = 2$ states at collision energies close to the $n = 2$ threshold and below the $n = 3$ threshold: ——, present results; — — —, 15-state R-matrix calculation (Aggarwal *et al* 1991); ●, experimental data (Williams 1988).

Table 1. Integral cross sections in units of πa_0^2 at collision energies between the $n = 2$ and $n = 3$ thresholds. Our results (RM2D) are compared with those of coupled-pseudostates (CPS, Callaway 1982), convergent close-coupling (CCC, Bray *et al* 1996), intermediate energy R-matrix (IERM, Odgers *et al* 1995, 1996), R-matrix with pseudostates (RMPS, Bartschat *et al* 1996) and 15-state R-matrix (RM15, Aggarwal *et al* 1991) calculations. In the CCC case, the cross sections were actually calculated at slightly different energies: the values below have been obtained by linear interpolation.

Energy (Ryd)		RM2D	CPS	CCC	IERM	RMPS	RM15
0.76	1s–1s	6.980	6.909	6.932		6.956	6.520
	1s–2s	0.135	0.136	0.135	0.136	0.135	0.149
	1s–2p	0.222	0.224	0.229	0.223	0.222	0.244
0.78	1s–1s	6.804	6.727	6.779		6.779	6.349
	1s–2s	0.148	0.149	0.149	0.149	0.148	0.166
	1s–2p	0.230	0.231	0.231	0.231	0.230	0.253
0.80	1s–1s	6.628	6.552	6.594		6.602	6.175
	1s–2s	0.175	0.176	0.182	0.176	0.175	0.196
	1s–2p	0.261	0.261	0.252	0.262	0.261	0.289
0.82	1s–1s	6.457	6.318	6.419		6.430	6.002
	1s–2s	0.198	0.200	0.192	0.199	0.199	0.221
	1s–2p	0.298	0.298	0.290	0.299	0.298	0.332
0.84	1s–1s	6.290	6.216	6.246		6.265	5.834
	1s–2s	0.210	0.212	0.208	0.211	0.211	0.233
	1s–2p	0.340	0.341	0.333	0.342	0.341	0.381
0.86	1s–1s	6.193	6.120	6.126		6.172	5.735
	1s–2s	0.164	0.166	0.173	0.165	0.165	0.180
	1s–2p	0.353	0.354	0.352	0.356	0.355	0.392
0.87	1s–1s	6.078	6.007	6.026		6.058	5.646
	1s–2s	0.198	0.199	0.187	0.199	0.197	0.225
	1s–2p	0.330	0.331	0.285	0.334	0.330	0.379
0.88	1s–1s	5.984	5.912	5.935		5.963	5.550
	1s–2s	0.220	0.222	0.223	0.221	0.221	0.245
	1s–2p	0.410	0.411	0.408	0.413	0.413	0.461

of Williams (1988). We also show the 15-state R-matrix results to illustrate the effect of not including pseudostates to represent highly excited states and the continuum of the target. We have not plotted the results of the CPS, CCC, IERM and RMPS calculations, as they would be indistinguishable from our own. Instead, a comparison at selected energies is made in table 1. We see that for excitation the agreement is within 3%, while for elastic scattering the differences are less than 1%.

To obtain resonance positions and widths, we perform a least-squares fit of the eigenphase sum to the usual Breit–Wigner form:

$$\delta(E) = \delta_0 + \delta_1 E + \tan^{-1}\left(\frac{\Gamma/2}{E_R - E}\right), \tag{8}$$

where E_R is the resonance energy (position), Γ is the width, and where we have assumed a linear variation of the background phase shift near the resonance. In order to fit resonances close to threshold, it was necessary to propagate the R-matrix in one dimension out to several hundred a_0. In table 2 we compare our values for the series of resonances converging to the $n = 3$ threshold with those obtained using the IERM (Odgers *et al* 1995), 15-state R-matrix (Pathak *et al* 1988) and CPS (Callaway 1982) calculations. In general there is very good agreement for the resonance positions, with some small but unimportant differences in the widths. Resonance positions have also been determined experimentally by Williams (1988)

Table 2. Energies E_r and widths Γ_r (in Ryd) of resonances below the $n = 3$ threshold of H ($E_{th} = 0.8889$ Ryd). The number in parentheses indicates the power of 10 by which the preceding quantity should be multiplied.

	Present		Odgers *et al* (1995)		Pathak *et al* (1988)		Callaway (1982)	
$^{(2S+1)}L^{\pi}$	E_r	Γ_r	E_r	Γ_r	E_r	Γ_r	E_r	Γ_r
$^1S^e$	0.861 98	2.84 (−3)	0.862 00	3.04 (−3)	0.861 987	3.01 (−3)	0.861 99	2.86 (−3)
	0.884 44	6.08 (−4)	0.884 57	5.99 (−4)	0.884 453	5.80 (−4)	0.884 45	6.11 (−4)
	0.887 72	1.71 (−4)	0.887 79	1.88 (−4)	0.887 739	1.49 (−4)	0.887 73	1.55 (−4)
	0.887 98	1.03 (−4)	0.888 01	6.50 (−5)	0.887 993	8.10 (−5)	0.887 99	6.74 (−5)
$^3S^e$	0.882 03	1.77 (−5)	0.882 09	2.02 (−5)	0.882 032	1.70 (−5)	0.882 03	1.77 (−5)
	0.887 52	4.30 (−6)	0.887 49		0.887 527		0.887 52	4.28 (−6)
$^1P^o$	0.751 34	1.55 (−3)			0.751 344	2.32 (−3)	0.751 21	1.47 (−3)
	0.874 56	2.38 (−3)	0.874 57	2.11 (−3)	0.874 574	2.51 (−3)	0.874 57	2.39 (−3)
	0.882 86	1.79 (−5)	0.882 62		0.882 857	1.80 (−5)	0.882 86	1.79 (−5)
	0.887 77	4.52 (−6)	0.887 81		0.887 710		0.887 77	4.36 (−6)
	0.888 19	1.42 (−4)	0.888 22	1.39 (−4)	0.888 194	1.33 (−4)	0.888 20	1.37 (−4)
$^3P^o$	0.864 18	3.26 (−3)	0.864 16	3.00 (−3)	0.864 173	3.43 (−3)	0.864 16	3.29 (−3)
	0.885 15	6.06 (−4)	0.885 17	4.98 (−4)	0.885 165	6.07 (−4)	0.885 16	6.11 (−4)
	0.887 24	8.49 (−6)	0.887 31		0.887 241	8.00 (−6)	0.887 24	8.39 (−6)
	0.888 18	1.27 (−4)	0.888 20	8.70 (−5)	0.888 185	1.13 (−4)	0.888 18	1.22 (−4)
	0.888 75	2.48 (−5)	0.888 44		0.888 753	2.40 (−5)		
$^1D^e$	0.868 02	3.33 (−3)	0.868 08	3.37 (−3)	0.868 099	3.14 (−3)	0.868 09	3.27 (−3)
	0.886 32	4.87 (−4)	0.886 43	4.85 (−4)	0.886 378	4.28 (−4)	0.886 36	4.83 (−4)
	0.888 50	4.26 (−5)	0.888 54	4.28 (−5)	0.888 428	4.30 (−5)	0.888 49	5.37 (−5)
$^3D^e$	0.882 07	7.49 (−4)	0.882 00	7.53 (−4)	0.882 090	7.72 (−4)	0.882 07	7.50 (−4)
	0.884 52	1.69 (−5)	0.884 65	1.60 (−5)	0.884 522	1.60 (−5)	0.884 53	1.70 (−5)
	0.888 21	3.18 (−6)	0.888 21		0.888 209		0.888 21	3.15 (−6)
$^1F^o$	0.886 88	1.05 (−5)	0.886 25		0.886 884	1.10 (−5)	0.886 89	1.00 (−5)
$^3F^o$	0.876 97	2.18 (−4)	0.877 01	2.23 (−4)	0.876 989	2.28 (−4)	0.876 97	2.18 (−4)
	0.887 99	1.00 (−5)	0.888 02	1.00 (−5)	0.887 999	1.10 (−5)	0.888 00	1.08 (−5)
$^1G^e$	0.887 53	1.05 (−3)	0.887 50	1.09 (−3)	0.887 493	9.52 (−4)		

from his measured 2s and 2p excitation cross sections, and by Warner *et al* (1990) from measurements of angular distributions for excitation into the $n = 2$ states. There is generally good agreement with the theoretical values presented in table 2.

We have also fitted the well known $^1P^o$ shape resonance just above threshold, using the form suggested by Callaway (1982) to describe the rapidly decreasing background close to threshold

$$\delta(E) = \delta_0 + \delta_1(E - E_{th}) + \tan^{-1}\left(\frac{\Gamma/2}{E_R - E}\right) + \frac{\delta_{-1}}{E - E_{th}}, \tag{9}$$

where E_{th} is the threshold energy. We obtain an energy of 0.751 34 Ryd and a width of 0.001 55 Ryd. Williams (1988) has estimated resonance parameters by fitting his measured excitation cross sections. From the 1s–2p cross section, he assigned to this resonance an energy of 0.751 33 Ryd and a width of 0.001 62 Ryd, while from the 1s–2s cross section he obtained an energy of 0.751 18 Ryd and a width of 0.001 54 Ryd.

Herrick and Sinanoglu (1975) and Cortés *et al* (1992) have also reported a $^3P^o$ shape resonance at 0.7514 Ryd and 0.7532 Ryd, respectively. We have not been able to find this resonance, and concur with Ho and Bhatia (1993) that if it exists, it must be very narrow.

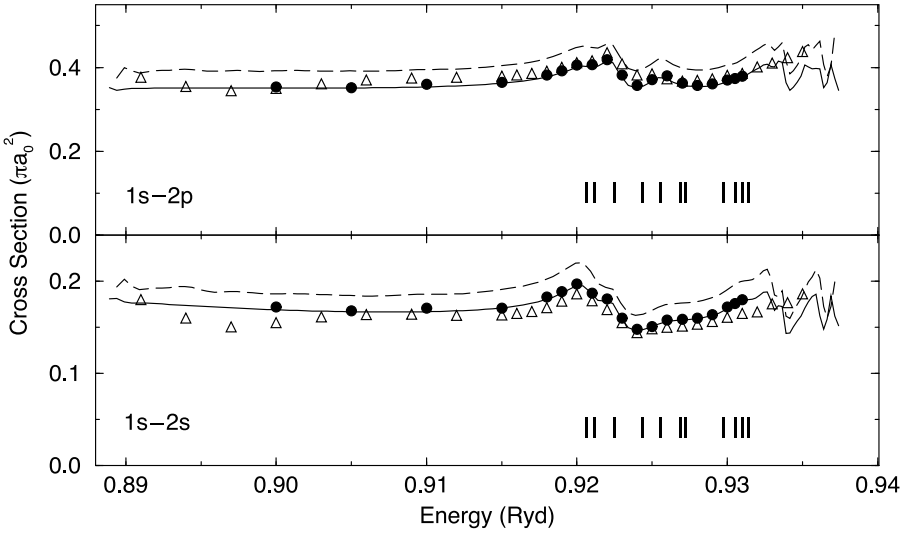

Figure 3. Integral cross sections for excitation of the ground state into the $n = 2$ states at collision energies between the $n = 3$ and $n = 4$ thresholds: ——, present results; — — —, 15-state R-matrix calculation (Aggarwal *et al* 1991); ●, coupled pseudostates calculation (Callaway 1988); △, J-matrix calculation (Konovalov and McCarthy 1994). The positions of the broadest resonances are indicated by vertical bars.

3.2. Between the $n = 3$ and $n = 4$ thresholds

While there is a wealth of theoretical and experimental data for electron–hydrogen scattering at collision energies up to the $n = 3$ threshold, there is considerably less between the $n = 3$ and $n = 4$ thresholds, in particular concerning the excitation of the $n = 3$ states. Of the various methods mentioned in the previous section, only the CPS (extended to 28 states, Callaway 1988), J-matrix (Konovalov and McCarthy 1994) and 15-state R-matrix (Aggarwal *et al* 1991) calculations have been extended to this energy range. (The IERM method has been used to calculate excitation cross sections into the $n = 3$ states, but at energies above the ionization threshold.) Callaway (1985) has also performed an 11-state CPS calculation for excitation into the $n = 2$ states, which yields similar results to his 28-state CPS calculation. We are not aware of any experimental results covering this energy range.

Integral cross sections for excitation into the $n = 2$ and $n = 3$ states are presented, respectively, in figures 3 and 4. Our results are in excellent agreement with those of the 28-state CPS calculation (Callaway 1988). There are some differences with the results of the J-matrix calculation of Konovalov and McCarthy (1994), particularly in the energy range between the $n = 3$ threshold and the lowest Feshbach resonances at approximately 0.92 Ryd. For transitions into the $n = 2$ states, our results are relatively smooth as a function of energy, whereas those of the J-matrix calculation tend to oscillate slightly. We also note some differences in magnitude, for example approximately 12% for the 1s–2s transition at 0.897 Ryd. These differences have also been commented upon by Fon *et al* (1995), who concluded that the J-matrix calculation may not have converged. Also shown in figures 3 and 4 are the results of the 15-state R-matrix calculation by Aggarwal *et al* (1991). While the form of these cross sections is similar to that of our results, they are consistently higher: for excitation into the $n = 2$ states the differences are of the order of 10–12%. For the 1s–3p transition, the differences are of the order of 15% while for the 1s–3d transition they vary between 5 and

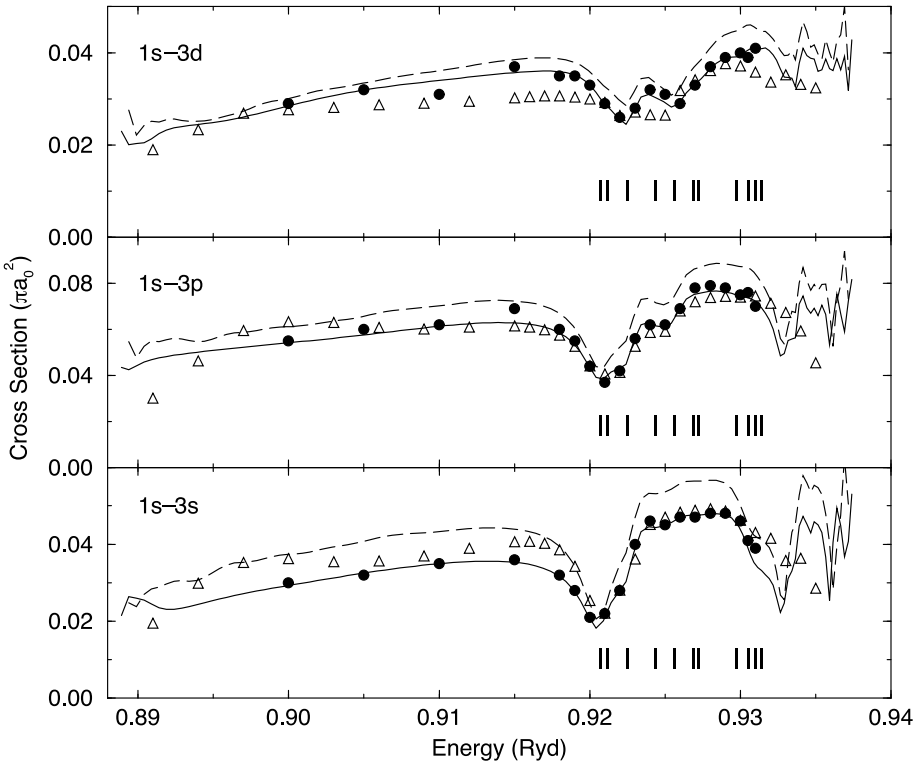

Figure 4. Integral cross sections for excitation of the ground state into the $n = 3$ states at collision energies between the $n = 3$ and $n = 4$ thresholds: ——, present results; — — —, 15-state R-matrix calculation (Aggarwal *et al* 1991); ●, coupled pseudostates calculation (Callaway 1988); △, J-matrix calculation (Konovalov and McCarthy 1994). The positions of the broadest resonances are indicated by vertical bars.

15%. The largest differences (20–25%) occur for the 1s–3s transition.

In table 3 we present parameters and widths for resonances below the $n = 4$ threshold. We compare our values with those of the 15-state R-matrix (Pathak *et al* 1988), complex coordinate rotation (Ho and Callaway 1986) and 28-state CPS (Callaway 1988) calculations. There is generally very good agreement, particularly with the extensive set of results obtained from the 15-state R-matrix calculation. The main differences concern the widths of the higher-lying resonances. We have been able to fit some of the resonances that were too narrow for Pathak *et al*. For a number of partial waves ($^3D^e$, $^1F^o$, $^3G^e$), we have found resonances that they did not find, including a relatively broad (1.07×10^{-4}) $^3D^e$ resonance at 0.937 17 Ryd. On the other hand, we did not find their narrow $^1P^o$ resonance at 0.937 377 Ryd.

We have indicated in figures 3 and 4 the positions of the broadest resonances (width $> 10^{-3}$ Ryd). Since several partial waves contribute to the cross section, it is generally not possible to assign one resonance to a particular feature.

Shape resonances just above the $n = 3$ threshold have been reported by a number of authors (Pathak *et al* 1988, Ho and Bhatia 1993, Bhatia and Ho 1994, Ho 1994). However the method of fitting the eigenphase sum was not able to provide reliable values for the resonance parameters, due to the rapidly decreasing background close to threshold. An alternative approach based on the time-delay matrix (Smith 1960) is currently being investigated.

Table 3. Energies E_r and widths Γ_r (in Ryd) of resonances below the $n = 4$ threshold of H ($E_{th} = 0.9375$ Ryd). The number in parentheses indicates the power of ten by which the preceding quantity should be multiplied.

	Present		Pathak *et al* (1988)		Ho and Callaway (1986)		Callaway (1988)	
$^{(2S+1)}L^{\pi}$	E_r	Γ_r	E_r	Γ_r	E_r	Γ_r	E_r	Γ_r
$^1S^e$	0.920 74	1.89 (−3)	0.920 784	2.19 (−3)	0.920 725	1.9 (−3)	0.920 7	2.0 (−3)
	0.930 61	1.64 (−3)	0.930 615	1.42 (−3)	0.930 55	1.76 (−3)	0.931 5	1.63 (−3)
	0.932 85	6.94 (−4)	0.932 950	5.40 (−4)				
	0.935 97	2.54 (−4)	0.936 010	1.86 (−4)				
	0.936 99	8.84 (−5)	0.936 967	9.00 (−5)				
	0.937 07	1.40 (−4)	0.937 081	7.10 (−5)				
	0.937 33	3.13 (−6)	0.937 325	2.60 (−5)				
$^3S^e$	0.931 09	3.52 (−5)	0.931 102	3.70 (−5)			0.931 11	3.7 (−5)
	0.935 46	1.49 (−5)	0.935 462	1.30 (−5)				
	0.936 43	1.51 (−5)	0.936 453	1.30 (−5)				
	0.936 83	5.25 (−6)	0.936 831					
	0.937 28	1.89 (−6)	0.937 278					
$^1P^o$	0.925 65	2.08 (−3)	0.925 739	2.49 (−3)	0.925 67	2.02 (−3)	0.925 7	2.7 (−3)
	0.931 42	4.43 (−5)	0.931 422	3.60 (−5)				
	0.935 30	4.67 (−4)	0.935 352	4.50 (−4)				
	0.935 60	1.58 (−5)	0.935 616	1.60 (−5)				
	0.936 77	1.12 (−5)	0.936 795					
	0.936 89	5.24 (−6)	0.936 893	9.30 (−5)				
	0.937 30	1.76 (−6)	0.937 297					
			0.937 377					
	0.937 39	2.37 (−5)	0.937 391					
$^3P^o$	0.921 26	2.02 (−3)	0.921 281	2.88 (−3)	0.921 28	2.04 (−3)	0.921 4	2.3 (−3)
	0.931 47	1.12 (−3)	0.931 495	9.77 (−4)	0.931 465	1.17 (−3)	0.932 0	1.0 (−3)
	0.933 23	9.71 (−4)	0.933 224	6.16 (−4)				
	0.933 91	3.47 (−5)	0.933 923	3.10 (−5)				
	0.936 10	2.65 (−4)	0.936 116	2.10 (−4)				
	0.936 71	9.49 (−6)	0.936 711					
	0.937 04	9.17 (−5)	0.937 048	7.00 (−5)				
	0.937 25	7.46 (−5)	0.937 267	4.70 (−5)				
	0.937 32	2.26 (−6)	0.937 321					
	0.937 35	3.22 (−5)	0.937 351	2.00 (−5)				
$^1D^e$	0.922 55	1.96 (−3)	0.922 492	2.51 (−3)	0.922 50	1.9 (−3)	0.922 6	2.5 (−3)
	0.931 05	1.35 (−3)	0.931 047	1.47 (−3)	0.931 02	1.52 (−3)		
	0.933 67	1.44 (−4)	0.933 659	4.21 (−4)	0.933 75	4.8 (−4)		
	0.933 74	3.67 (−4)	0.933 887	5.44 (−4)				
	0.934 66	3.25 (−5)	0.934 676	2.70 (−5)				
	0.936 34	2.19 (−4)	0.936 370	2.00 (−5)				
	0.936 95	8.37 (−6)	0.936 951	1.50 (−5)				
	0.937 14	3.90 (−5)	0.937 379	1.50 (−5)				
	0.937 39	1.33 (−6)	0.937 392					
$^3D^e$	0.926 97	2.09 (−3)	0.926 761	2.83 (−3)	0.926 85	2.1 (−3)	0.925 9	2.0 (−3)
	0.932 07	3.91 (−5)	0.932 075	3.80 (−5)				
	0.935 82	4.95 (−4)	0.935 711	5.36 (−4)				
	0.935 89	2.00 (−5)	0.935 869	1.89 (−4)				
	0.936 57	1.46 (−5)	0.936 578	1.40 (−5)				
	0.937 01	5.28 (−6)	0.937 008	6.40 (−5)				
	0.937 17	1.07 (−4)						
	0.937 34	1.62 (−5)						

Table 3. (Continued)

	Present		Pathak *et al* (1988)		Ho and Callaway (1986)		Callaway (1988)	
$^{(2S+1)}L^{\pi}$	E_r	Γ_r	E_r	Γ_r	E_r	Γ_r	E_r	Γ_r
$^1F^o$	0.929 79	1.30 (−3)	0.929 804	1.31 (−3)	0.929 75	1.3 (−3)	0.9297	1.3 (−3)
	0.933 07	4.23 (−5)	0.933 089	3.60 (−5)				
	0.936 31	1.46 (−5)	0.936 308	1.30 (−5)				
	0.936 59	1.64 (−4)	0.936 678	9.70 (−5)				
	0.937 16	4.12 (−6)						
	0.937 37	2.88 (−5)						
$^3F^o$	0.924 43	2.95 (−3)	0.924 418	2.79 (−3)	0.924 4	2.9 (−3)	0.9247	2.4 (−3)
	0.934 70	4.24 (−4)	0.934 518	6.64 (−4)	0.934 72	6.0 (−4)		
	0.934 73	3.36 (−4)	0.934 853	4.84 (−4)				
	0.935 78	2.01 (−5)	0.935 800	1.20 (−5)				
	0.936 71	2.50 (−4)	0.936 721	1.86 (−4)				
	0.937 25	5.35 (−6)	0.937 249					
	0.937 28	8.02 (−5)	0.937 285	7.10 (−5)				
$^1G^e$	0.927 28	1.45 (−3)	0.927 325	1.56 (−3)				
	0.935 62	3.35 (−4)	0.935 660	2.63 (−4)				
	0.937 02	1.61 (−5)	0.937 045	1.60 (−5)				
	0.937 06	8.44 (−5)	0.937 062	6.30 (−5)				
$^3G^e$	0.934 29	2.69 (−4)	0.934 347	2.56 (−4)				
	0.934 48	6.98 (−5)	0.934 490	5.80 (−5)				
	0.936 80	9.74 (−6)	0.936 805					
	0.937 33	2.64 (−6)						
	0.937 35	8.63 (−6)	0.937 358	1.30 (−5)				

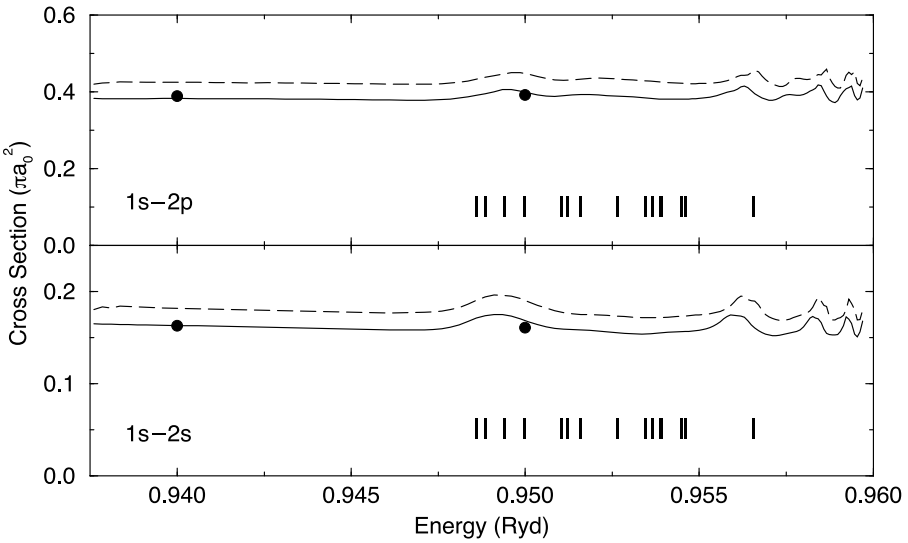

Figure 5. Integral cross sections for excitation of the ground state into the $n = 2$ states at collision energies between the $n = 4$ and $n = 5$ thresholds: ——, present results; — — —, 15-state R-matrix calculation (Aggarwal *et al* 1991); ●, coupled pseudostates calculation (Callaway 1985). The positions of the broadest resonances are indicated by vertical bars.

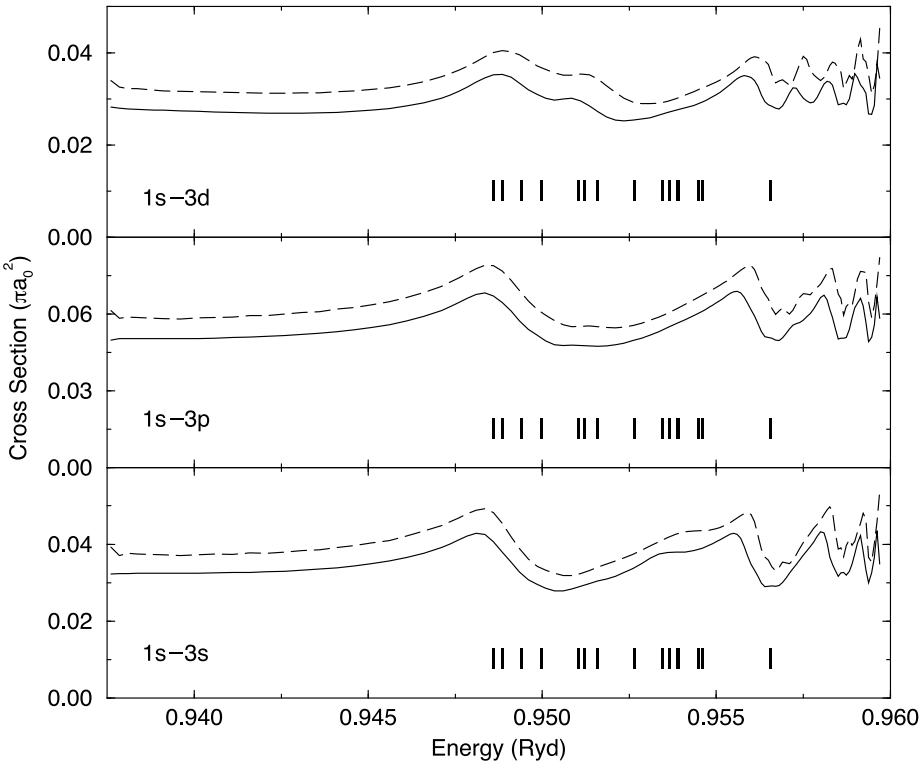

Figure 6. Integral cross sections for excitation of the ground state into the $n = 3$ states at collision energies between the $n = 4$ and $n = 5$ thresholds: ——, present results; — — —, 15-state R-matrix calculation (Aggarwal *et al* 1991). The positions of the broadest resonances are indicated by vertical bars.

3.3. Between the $n = 4$ and $n = 5$ thresholds

There are at present very few data available at these collision energies, particularly for excitation into the $n \geqslant 3$ states. Callaway (1985) has performed an 11-state CPS calculation, considering only excitation into the 2s and 2p states. Two of his data points lie in the current energy range and are plotted in figure 5, together with our results. The agreement is very good, the differences being of the order of 1 or 2%.

The only other work we are aware of that provides cross sections for excitation in this energy range is the 15-state R-matrix calculation of Aggarwal *et al* (1991). We compare with the results of this calculation in figures 5–7. In general the shapes of the cross sections as a function of collision energy are similar, although resonances in the 15-state R-matrix results lie at slightly higher energies. This is particularly evident for excitation into the $n = 4$ states (figure 7), and may be attributed to the absence of states with principal quantum number $n > 5$ in the 15-state R-matrix calculation. As at lower energies, there are differences in magnitude due to the lack of pseudostates representing highly excited states and the continuum of the target. For excitation into the $n = 2$ states, these differences are of the order of 10–12%, while for the $n = 3$ states they are of the order of 15–20%. The largest differences (20–30%) occur for the 1s–4s transition, with differences of 10–20% for excitation into the other $n = 4$ states.

In table 4 we compare our resonance parameters with those obtained using the complex

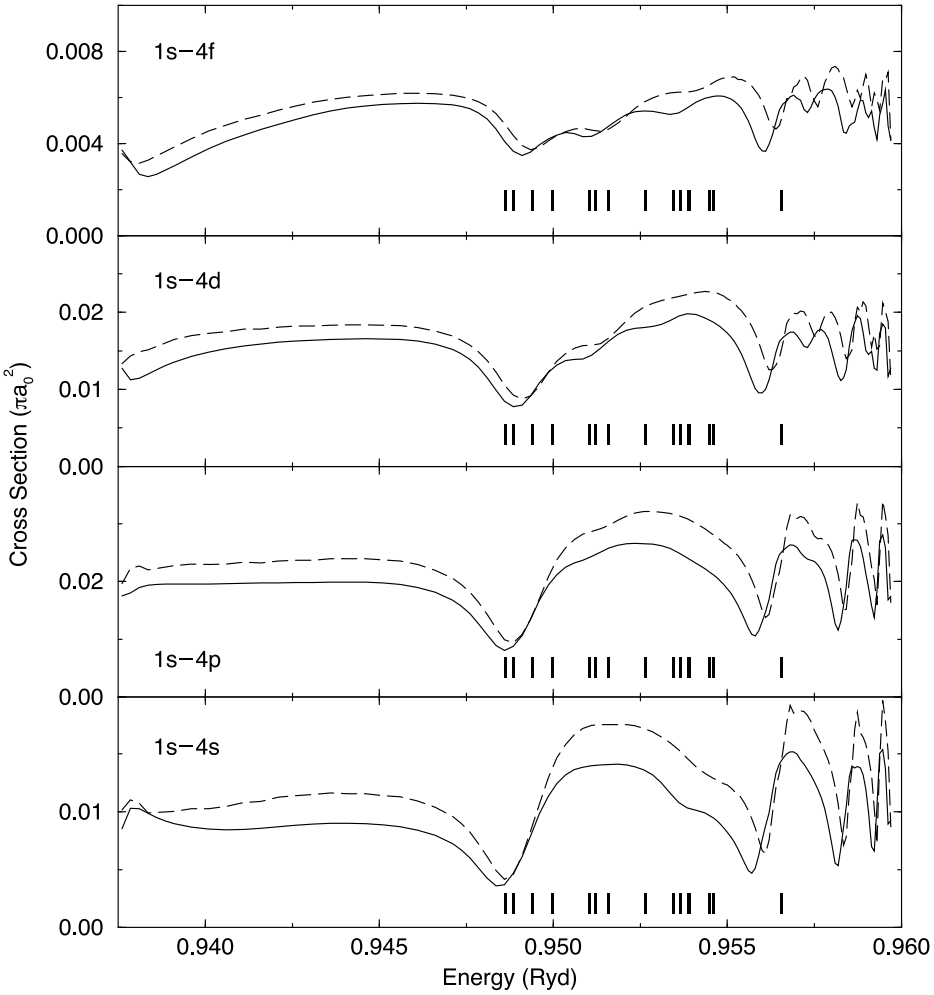

Figure 7. Integral cross sections for excitation of the ground state into the $n = 4$ states at collision energies between the $n = 4$ and $n = 5$ thresholds: ——, present results; — — —, 15-state R-matrix calculation (Aggarwal *et al* 1991). The positions of the broadest resonances are indicated by vertical bars.

coordinate rotation method (Ho and Callaway 1986). These authors reported positions and widths for only the lowest resonance in a given series. In general, the agreement is once again very good, except for a few narrow resonances with large angular momentum.

4. Conclusions

We have presented integral cross sections and resonance parameters for electron-impact excitation of hydrogen at collision energies up to the $n = 5$ threshold. Between the $n = 2$ and $n = 4$ thresholds, there is generally very good agreement with the results of other accurate theoretical work and experiment. Above the $n = 4$ threshold, there are very few other data, particularly for excitation into the higher lying states. The 2D R-matrix propagator has been able to furnish extensive and, we believe, precise results for these processes. This

Table 4. Energies E_r and widths Γ_r (in Ryd) of resonances below the $n = 5$ threshold of H ($E_{th} = 0.9600$ Ryd). The number in parentheses indicates the power of ten by which the preceding quantity should be multiplied.

	Present		Ho and Callaway (1986)	
$^{(2S+1)}L^{\pi}$	E_r	Γ_r	E_r	Γ_r
$^1S^e$	0.948 64	1.38 (−3)	0.948 6	1.4 (−3)
	0.953 48	1.54 (−3)	0.953 35	1.3 (−3)
	0.955 86	6.71 (−4)		
	0.958 20	3.33 (−4)		
	0.958 63	3.89 (−4)		
	0.959 23	1.59 (−4)		
	0.959 62	1.10 (−4)	0.959 58	2.8 (−4)
$^3S^e$	0.954 59	4.57 (−5)		
	0.957 74	3.99 (−5)		
	0.957 81	2.90 (−5)		
$^1P^o$	0.951 07	1.50 (−3)	0.950 90	1.5 (−3)
	0.954 74	4.68 (−5)		
	0.956 76	8.41 (−4)	0.956 25	1.2 (−3)
	0.959 11	1.33 (−5)		
$^3P^o$	0.948 88	1.40 (−3)	0.948 8	1.4 (−3)
	0.953 93	1.36 (−3)	0.953 45	1.3 (−3)
	0.955 87	7.43 (−4)		
	0.959 27	1.60 (−4)		
$^1D^e$	0.949 43	1.46 (−3)	0.949 25	1.3 (−3)
	0.953 68	1.13 (−3)	0.953 5	1.4 (−3)
	0.954 51	2.06 (−3)	0.954 4	1.4 (−3)
	0.956 52	5.67 (−5)		
	0.959 62	1.35 (−5)	0.959 66	6.0 (−4)
$^3D^e$	0.951 61	1.27 (−3)	0.951 5	1.3 (−3)
	0.957 82	7.94 (−5)	0.957 36	6.0 (−4)
	0.958 03	3.26 (−5)		
	0.958 37	1.09 (−4)		
	0.959 66	8.90 (−6)		
	0.959 67	6.69 (−6)		
$^1F^o$	0.952 68	1.44 (−3)	0.952 46	1.45 (−3)
	0.955 49	4.83 (−5)		
	0.956 58	1.15 (−3)	0.956 28	1.0 (−3)
	0.958 28	3.58 (−5)		
	0.958 38	5.92 (−5)		
	0.958 84	5.45 (−5)	0.958 8	6.0 (−4)
$^3F^o$	0.950 01	1.37 (−3)	0.949 92	1.3 (−3)
	0.954 64	1.31 (−3)	0.954 43	1.24 (−3)
	0.955 86	7.48 (−4)	0.955 35	7.5 (−4)
	0.957 06	6.67 (−5)		
	0.958 74	3.36 (−4)		
$^1G^e$	0.951 23	1.50 (−3)	0.951 15	1.5 (−3)
	0.956 64	8.78 (−4)	0.956 26	1.0 (−3)
	0.957 31	5.67 (−4)	0.957 30	4 (−4)
	0.957 69	1.01 (−4)		
	0.958 30	2.65 (−4)		
	0.959 00	2.30 (−4)		
	0.959 40	1.04 (−5)	0.959 50	9 (−4)

Table 4. (Continued)

	Present		Ho and Callaway (1986)	
$^{(2S+1)}L^{\pi}$	E_r	Γ_r	E_r	Γ_r
$^3G^e$	0.953 94	1.42 (−3)	0.953 45	1.25 (−3)
	0.956 12	6.01 (−5)		
	0.958 60	3.10 (−5)	0.958 5	9 (−4)
	0.959 10	2.24 (−5)		

is made possible by the accurate treatment of an extended region of configuration space by partitioning into a number of sub-regions. A more rigorous test of the method will be to compare detailed quantities such as angular distributions and asymmetry parameters. We also intend to study excitation of even higher-lying states of hydrogen, which are needed for astrophysical applications.

Acknowledgments

We would like to thank Klaus Bartschat and Igor Bray for providing their data in tabular form. All computation was performed on an IBM SP2 at the Centre National Universitaire Sud de Calcul, Montpellier, France with time allocated to the project LSA 2538, and on local IBM workstations partially financed by the Conseil Régional de Bretagne, the Conseil Général d'Ille et Vilaine and the District de Rennes.

References

Aboudarham J, Berrington K A, Callaway J, Feautrier N, Hénoux J C, Peach G and Saraph H E 1992 *Astron. Astrophys.* **262** 302–7
Aggarwal K M, Berrington K A, Burke P G, Kingston A E and Pathak A 1991 *J. Phys. B: At. Mol. Opt. Phys.* **24** 1385–410
Bartschat K, Bray I, Burke P G and Scott M P 1996 *J. Phys. B: At. Mol. Opt. Phys.* **29** 5493–503
Bhatia A K and Ho Y K 1994 *Phys. Rev.* **50** 4886–90
Bray I, McCarthy I E and Stelbovics A T 1996 *J. Phys. B: At. Mol. Opt. Phys.* **29** L245–7
Bray I and Stelbovics A T 1992 *Phys. Rev.* A **46** 6995–7011
Burke V M and Noble C J 1995 *Comput. Phys. Commun.* **85** 471–500
Callaway J 1982 *Phys. Rev.* A **26** 199–208
——1988 *Phys. Rev.* A **37** 3692–6
Cortés M, Macías A, Martin F and Riera A 1992 *J. Phys. B: At. Mol. Opt. Phys.* **25** 83–96
Dunseath K M, Le Dourneuf M, Terao-Dunseath M and Launay J-M 1996 *Phys. Rev.* A **54** 561–72
Dunseath K M, Terao-Dunseath M, Le Dourneuf M and Launay J-M 1997 *J. Phys. B: At. Mol. Opt. Phys.* **30** L865–71
Fon W C, Ratnavelu K and Aggarwal K M 1994 *Phys. Rev.* A **49** 1786–96
Gailitis M 1976 *J. Phys. B: At. Mol. Phys.* **9** 843–54
Herrick D R and Sinanoglu O 1975 *Phys. Rev.* A **11** 97–110
Ho Y K 1994 *Phys. Lett.* A **189** 374–8
Ho Y K and Bhatia A K 1993 *Phys. Rev.* A **48** 3720–4
Ho Y K and Callaway J 1986 *Phys. Rev.* A **34** 130–7
Konovalov D A and McCarthy I E 1994 *J. Phys. B: At. Mol. Opt. Phys.* **27** L741–7
Light J C and Walker R B 1976 *J. Chem. Phys.* **65** 4272–82
Odgers B R, Scott M P and Burke P G 1995 *J. Phys. B: At. Mol. Opt. Phys.* **28** 2973–84
——1996 *J. Phys. B: At. Mol. Opt. Phys.* **29** 4320–1
Pathak A, Kingston A E and Berrington K A 1988 *J. Phys. B: At. Mol. Opt. Phys.* **21** 2939–51
Scholz T, Scott M P and Burke P G 1988 *J. Phys. B: At. Mol. Opt. Phys.* **21** L139–45
Shertzer J and Botero J 1994 *Phys. Rev.* A **49** 3673–9

Smith F T 1960 *Phys. Rev.* **118** 349–56
Wang Y D and Callaway J 1994 *Phys. Rev.* A **50** 2327–40
Warner C D, Rutter P M and King G C 1990 *J. Phys. B: At. Mol. Opt. Phys.* **23** 93–8
Williams J F 1988 *J. Phys. B: At. Mol. Opt. Phys.* **21** 2107–16